



Communication

# Relative Nuclease Resistance of a DNA Aptamer Covalently Conjugated to a Target Protein

Yudai Tabuchi <sup>1</sup>, Jay Yang <sup>1,2,3,\*</sup> and Masumi Taki <sup>1,4,\*</sup>

<sup>1</sup> Department of Engineering Science, Graduate School of Informatics and Engineering,

University of Electro-Communications (UEC), Chofu 182-8585, Japan; t1833099@gmail.com

<sup>2</sup> School of Medicine and Public Health, University of Wisconsin, Madison, WI 53706, USA

<sup>3</sup> Department of GI Surgery II, Graduate School of Medicine, Hokkaido University, Sapporo 068-8638, Japan

<sup>4</sup> Institute for Advanced Science, University of Electro-Communications (UEC), Chofu 182-8585, Japan

\* Correspondence: jyang75@wisc.edu (J.Y.); taki@pc.uec.ac.jp (M.T.)

**Abstract:** A major obstacle to the therapeutic application of an aptamer is its susceptibility to nuclease digestion. Here, we confirmed the acquisition of relative nuclease resistance of a DNA-type thrombin binding aptamer with a warhead (TBA<sub>3</sub>) by covalent binding to a target protein in the presence of serum/various nucleases. When the thrombin-inhibitory activity of TBA<sub>3</sub> on thrombin was reversed by the addition of the complementary strand, the aptamer was instantly degraded by the nucleases, showing that the properly folded/bound aptamer conferred the resistance. Covalently binding aptamers possessing both a prolonged drug effect and relative nuclease resistance would be beneficial for in vivo translational applications.

**Keywords:** covalent aptamer; nuclease resistance; sulfur (VI) fluoride exchange reaction (SuFEx); targeted covalent inhibitor (TCI); middle-molecule covalent drug; covalent biologics; complementary-strand (CS) antidote; reversing adverse drug effects (ADEs); aryl-sulfonyl fluoride warhead



**Citation:** Tabuchi, Y.; Yang, J.; Taki, M. Relative Nuclease Resistance of a DNA Aptamer Covalently Conjugated to a Target Protein. *Int. J. Mol. Sci.* **2022**, *23*, 7778. <https://doi.org/10.3390/ijms23147778>

Academic Editor: Bruno Pagano

Received: 8 June 2022

Accepted: 12 July 2022

Published: 14 July 2022

**Publisher's Note:** MDPI stays neutral with regard to jurisdictional claims in published maps and institutional affiliations.



**Copyright:** © 2022 by the authors. Licensee MDPI, Basel, Switzerland. This article is an open access article distributed under the terms and conditions of the Creative Commons Attribution (CC BY) license (<https://creativecommons.org/licenses/by/4.0/>).

## 1. Introduction

Modifications of the molecular structures of nucleic-acid aptamers [1–8] by incorporation of a non-natural phosphorothioate backbone and manipulation of the sugar or 5'-end structure are often used to reduce rapid hydrolysis by nucleases and to increase the in vivo circulation half-life [1,8,9]. It has also been suggested that unmodified natural DNA aptamers can be protected from hydrolysis by nucleases when they are tightly bound to target proteins. This nuclease-resistant property of a bound aptamer has been exploited to speed up the SELEX process for identifying an aptamer with the desired target specificity. A recent paper reported that an aptamer covalently bound to thrombin through a proximity-driven reaction conferred resistance to degradation by serum [10]. These observations are consistent with the idea that the nuclease resistance of a DNA aptamer depends on its affinity to the target protein [11–15]. However, whether the nuclease resistance of an aptamer depends on the exact chemistry of its covalent binding to the target remains unknown.

We recently reported on the creation of a covalently binding DNA aptamer by introducing a SO<sub>2</sub>F warhead (i.e., a reactive group) into designated positions on an aptamer [16]. This method differs from the previously reported inverse nucleophile reaction [10]. The warhead-modified covalently binding aptamer forms a permanent bond to a target protein with a dissociation constant ( $K_D$ ) rate of effectively zero, resulting in a left-shifted concentration-dependent inhibition activity. Here, we show that the covalently binding DNA aptamer also confers relative nuclease resistance to serum and to other specific nucleases (Figure 1). However, the nuclease sensitivity of the covalently bound aptamer returns with the addition of the complementary-strand antidote DNA, suggesting that the binding of the aptamer to the target confers the nuclease resistance and not the covalent-conjugation per se (Figure S1).

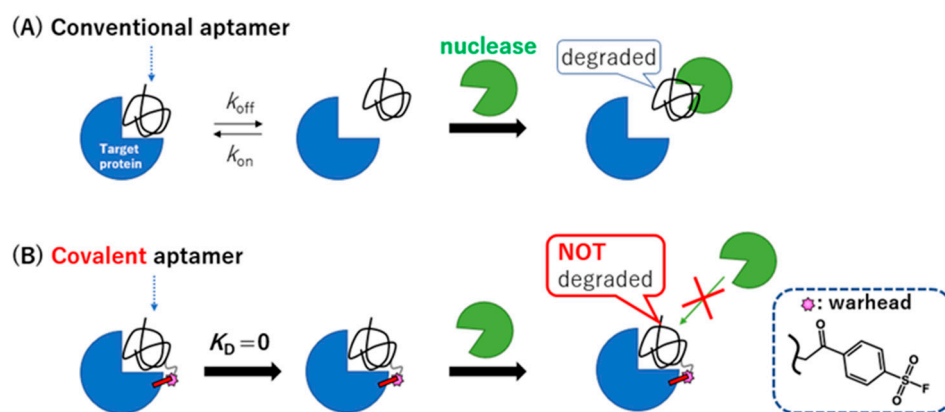


**Figure 1.** Susceptibility mechanism for the hydrolysis mediated by nucleases. (A) Conventional DNA aptamer: the aptamer (folded string) binds to its target protein (blue) (left). The aptamer dissociates from the target protein (middle). The free state of the aptamer is recognized by the nucleases (right). (B) Covalently binding DNA aptamer: a warhead-modified aptamer (pink star) forms a covalent bond (left) and permanently binds to the target protein (middle), which causes a semi-permanent nuclease resistance (right).

## 2. Results and Discussion

### 2.1. Kinetics of Thrombin Inhibition by TBA<sub>3</sub> Are Consistent with a Two-Step Process

As described previously, we introduced the SO<sub>2</sub>F warhead, which can react with any nucleophilic amino acid residues (i.e., serine, threonine, lysine, tyrosine, cysteine, and histidine) [17–24], into the 3rd thymine residue from the 5′-end of the thrombin binding aptamer (TBA), to create the covalently binding TBA (TBA<sub>3</sub>) [16]. We had previously deduced that TBA<sub>3</sub> is covalently bound to Y88 and H91 residues of thrombin through an LC-MS/MS analysis of trypsin digest fragments [16]. Here, we hypothesize that TBA<sub>3</sub> reversibly binds to thrombin prior to forming an irreversible covalent bond. This type of two-step process is observed for many known conventional covalent drugs [25–31] (Figure 2A). First, we demonstrated that TBA<sub>3</sub> showed a time-dependent inhibition activity, which supports the hypothesized two-step process (Figure 2B). If the irreversible covalent binding step preceded the rapid reversible equilibrium binding (i.e., a pseudo-first-order irreversible binding reaction), the  $k_{\text{obs}}$  vs. TBA<sub>3</sub> concentration plot would be linear (Scheme A, Figure 9.2 in [32]). TBA<sub>3</sub> showed a calculated  $k_{\text{inact}}/K_{\text{I}}$  value of  $(2.1 \pm 0.6) \times 10^5 \text{ M}^{-1}\text{s}^{-1}$ , which was of the same order as clinically approved covalent drugs (Figure 2C) [33].

### 2.2. TBA<sub>3</sub> Covalently Bound to Thrombin Resists Degradation by Human Serum

Next, we evaluated the nuclease resistance of TBA<sub>3</sub> in the presence of human serum or DNases. As a preliminary experiment, the hydrolysis of unmodified TBA was monitored by HPLC. After the serum treatment of TBA in the presence of thrombin, the original TBA peak completely disappeared, and a low-molecular-weight nucleotide peak was detected at the void volume (Figure 3A). As expected, unmodified TBA with a finite off rate dissociated from the target thrombin and was digested by the nucleases in the human serum. Since monitoring the hydrolysis of TBA<sub>3</sub> covalently conjugated to thrombin by HPLC is problematic, we followed a mobility shift of thrombin due to the covalent binding with TBA<sub>3</sub> by SDS-PAGE. Thrombin incubated with TBA<sub>3</sub> resulted in a persistent mobility shift on the gel electrophoresis, where the protein bands were visualized by CBB staining. The shifted band persisted even after incubation with the human serum for 24 h (Figure 3B), which suggests that TBA<sub>3</sub> covalently bound to thrombin resisted nuclease digestion.

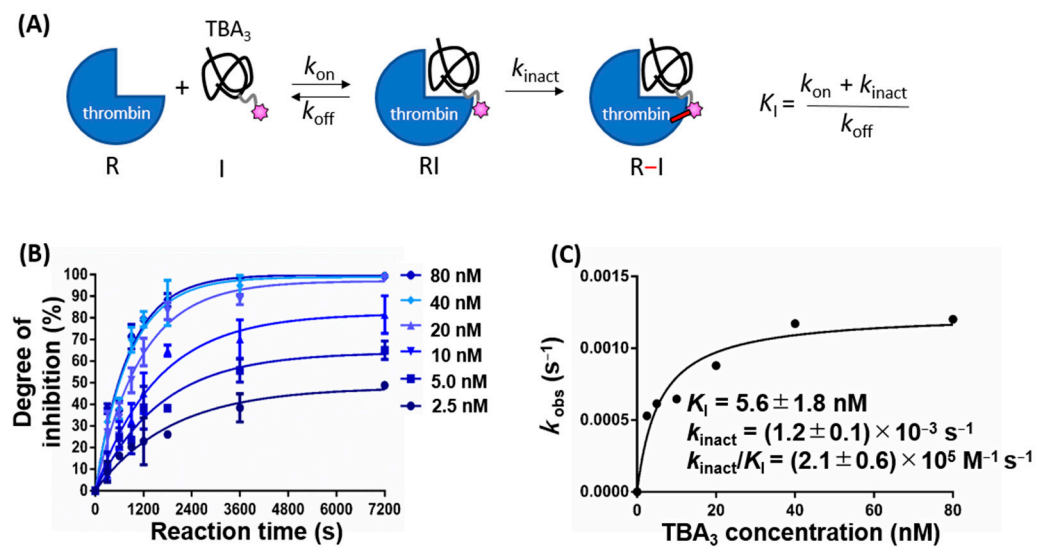


**Figure 2.** (A) Reaction kinetics of TBA<sub>3</sub>: a reversible interaction between TBA<sub>3</sub> and thrombin is described in terms of rate constants of association ( $k_{on}$ ) and dissociation ( $k_{off}$ ). Inactivation rate of thrombin by the covalent binding of TBA<sub>3</sub> is described as  $k_{inact}$ . The resulting  $k_{inact}:K_I$  ratio is preferred for ranking the potency of covalent inhibitors against a target, rather than using IC<sub>50</sub> values [31]. (B) Thrombin inhibition at each reaction time was monitored via a turbidimetric assay for different concentrations of TBA<sub>3</sub>. The pseudo-first-order rate constant  $k_{obs}$  was calculated for each TBA<sub>3</sub> concentration using nonlinear regression analysis in GraphPad Prism 6. (C) The obtained  $k_{obs}$  values were plotted against each covalent binder concentration to afford the second-order rate constant  $k_{inact}/K_I$ .

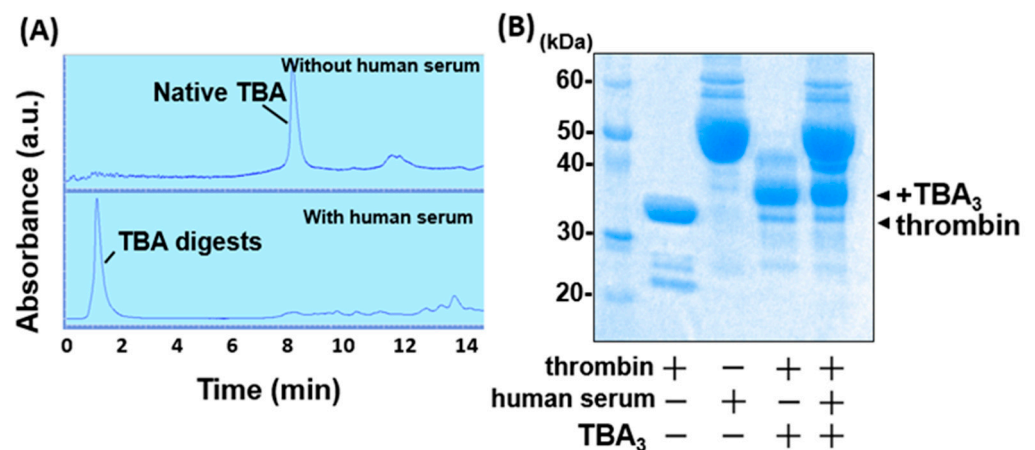


**Figure 3.** Nuclease resistance of unmodified TBA and TBA<sub>3</sub> in the presence of human serum. (A) LC absorbance profiles of unmodified TBA incubated with thrombin in the absence/presence of human serum. (B) Nuclease resistance of TBA<sub>3</sub> in the presence of human serum, confirmed by 12% (*w/v*) SDS-PAGE. Whole proteins were visualized by CBB staining. The band density of TBA<sub>3</sub>-conjugated thrombin (abbreviated as + TBA<sub>3</sub>) did not change after serum incubation for 24 h at 37 °C.

### 2.3. TBA<sub>3</sub> Covalently Bound to Thrombin Resists Degradation by Both Exonucleases and Endonucleases

To assess the nuclease resistance mechanism, we used several purified exonucleases and endonucleases instead of the human serum in further experiments. The nuclease resistance of unmodified TBA or TBA<sub>3</sub> was evaluated by native PAGE and SDS-PAGE, which reflect the bound and the covalently conjugated states of the aptamer/thrombin (e.g., 'RI' and 'R-I' states in Figure 2A), respectively. The bands corresponding to TBA-thrombin disappeared when treated with all nucleases, whereas those of TBA<sub>3</sub>-thrombin

did not (Figure 4). TBA<sub>3</sub> induced two distinct mobility shifts corresponding to the TBA<sub>3</sub> monoadduct and bisadduct via the covalent conjugation. For the bisadduct, two equimolar TBA<sub>3</sub> moieties were probably conjugated to different residues of thrombin, while both TBA<sub>3</sub> moieties seemed to recognize the same TBA-binding site [16]. In the presence of nucleases, the monoadduct band remained dense, whereas that of the bisadduct was largely eliminated. This suggests that while one of the conjugated TBA<sub>3</sub> moieties was in the bound state on thrombin, the other one was microscopically in the unbound state and was recognized by the nucleases (Figure S1, right). The conjugated bisadduct was equally digested with DNase I and S1 endonucleases, or with Exo VII exonuclease (Figure 4), suggesting that TBA<sub>3</sub> even microscopically displaced from the thrombin binding pocket was no longer afforded steric hindrance and was recognized by the nucleases, similarly to unmodified TBA.

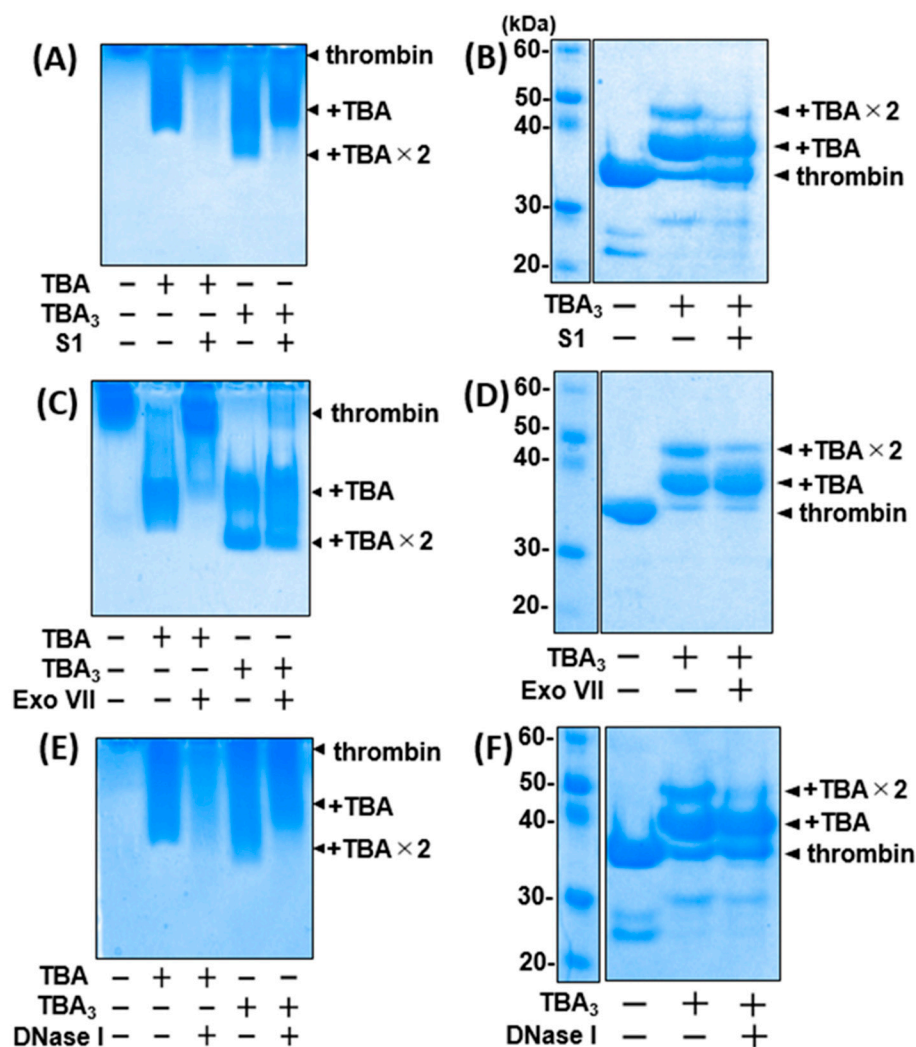


**Figure 4.** Nuclease resistances of unmodified TBA and TBA<sub>3</sub> against S1 (A,B), Exo VII (C,D), or DNase I (E,F) nucleases were confirmed by 12% native PAGE (left) and SDS-PAGE (right), respectively. Each nuclease treatment was performed for 24 h at 37 °C, and whole proteins were visualized using CBB staining. TBA monoadduct and bisadduct on thrombin are abbreviated as +TBA and +TBA × 2, respectively.

#### 2.4. The Complementary-Strand Antidote Restores the Nuclease Sensitivity

A unique and highly desirable property of the aptamer drug is its inherent reversibility via the addition of the CS antidote. We have previously shown that the inhibition of the thrombin enzymatic activity by TBA<sub>3</sub> is reversed by the CS [16], and here we investigated the effect of the CS on the nuclease resistance of TBA<sub>3</sub>. The addition of the CS resulted

in a further mobility shift of the TBA<sub>3</sub>-conjugated thrombin band in SDS-PAGE (Figure 5, middle), indicating that the CS formed a double strand with the thrombin-conjugated TBA<sub>3</sub>. The density of the shifted bands was reduced when treated with DNA duplex-specific nucleases (i.e., Exonuclease III and DNase I) (Figure 5, right). This indicated that the CS-hybridized double-stranded TBA<sub>3</sub> became unbound and was hydrolyzed by the nucleases even while covalently tethered to thrombin (Figure S1, bottom). Direct DNA staining of the gel confirmed the presence of the aptamer in the mobility-shifted bands and a loss of staining upon treatment with DNase I (Figure S2).

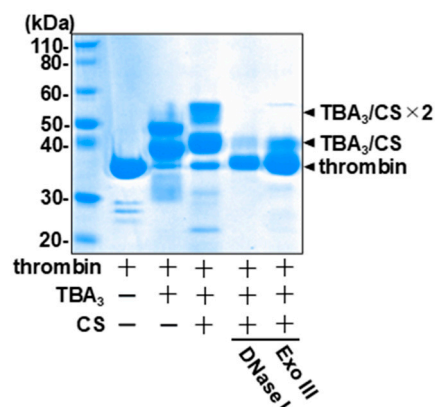


**Figure 5.** DNase I or Exo III nuclease susceptibility of double-stranded TBA<sub>3</sub> with the complementary strand (CS) was confirmed by 12% SDS-PAGE. Each nuclease treatment was performed for 24 h at 37 °C, and whole proteins were visualized using CBB staining.

### 2.5. Sustained Inhibition of Thrombin Activity by TBA<sub>3</sub> in the Presence of Nucleases

Finally, thrombin inhibition by unmodified TBA and TBA<sub>3</sub> in the presence of nucleases or human serum was monitored by a time-dependent change in optical density at 288 nm (i.e., a turbidimetric assay), which corresponds to thrombin-induced fibrin aggregation [16]. The thrombin inhibition activity of unmodified TBA was decreased when incubated with the nucleases or human serum, whereas that of TBA<sub>3</sub> was not (Figure 6). This indicates that TBA<sub>3</sub> resisted nuclease digestion and maintained the target inhibition activity when covalently bound to the target protein.

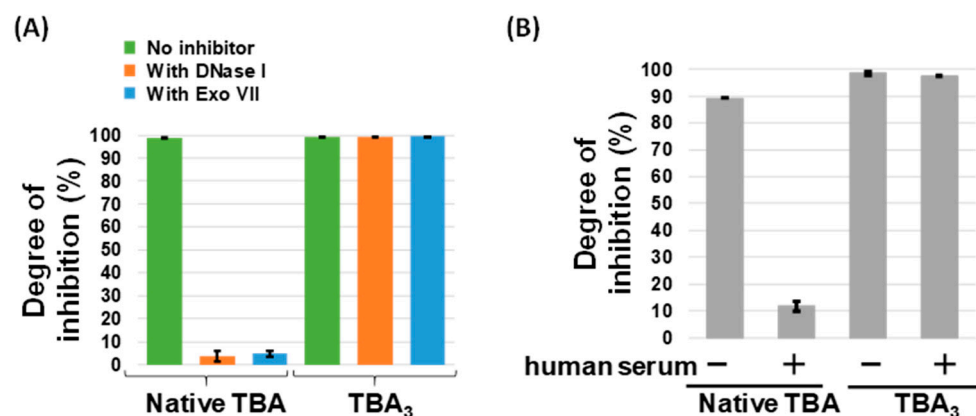


**Figure 6.** Comparison of thrombin inhibition activity between unmodified TBA and TBA<sub>3</sub> via the turbidimetric assay. (A) Thrombin inhibition activity of each aptamer in the presence of DNase I or Exo VII nuclease. The maximum absorbance (288 nm) of fibrin polymerization at 0 s was normalized to 0%. (B) Thrombin inhibition activity of each aptamer in the presence of human serum. Inhibition was calculated as above in (A).

### 3. Materials and Methods

#### 3.1. Chemicals and Reagents

All the reagents and solvents were purchased commercially and used without further purification, including human  $\alpha$ -thrombin (Haematologic Technologies Inc., #HCT-0020, Essex Junction, VT, USA), fibrinogen from human plasma (Aldrich, #9001-32-5, St. Louis, MO, USA), human serum (Sigma, #H4522, St. Louis, MO, USA), Exonuclease III (NEB, #M0206S, Ipswich, MA, USA), Exonuclease VII (NEB, #M0379S, USA), S1 nuclease (Takara, #2410A, Shiga, Japan), and DNase I (Nippon Gene, #314-08071, Tokyo, Japan). Thrombin binding aptamer (TBA): 5'-GGTTGGTGTGGTTGG-3', alkyne-containing TBA (T<sub>3</sub>): 5'-GGXTGGTGTGGTTGG-3' (X indicates a 5-Octadynyl-dU possessing a long spacer and a terminal alkyne replacing the thymine residue), and the complementary strand (CS) of TBA: 5'-CCAACCACACCAACC-3' were synthesized by Integrated DNA Technologies (IDT) Inc. (Coralville, IA, USA).

#### 3.2. High-Pressure Liquid Chromatography (HPLC) Analysis

A small-scale quantitative analysis of aptamers was carried out using a reverse-phase semi-micro HPLC system (PU-2085 with a C18 TSKgel column, JASCO with Tosoh #21813, Tokyo, Japan) connected to a photodiode array (PDA) detector. The aptamers were separated using a 0–60% gradient of acetonitrile containing a 20 mM triethylamine acetate aqueous solution (pH 7.4) for 26 min at a flow rate of 200  $\mu$ L per minute.

#### 3.3. Image Capturing

All images of stained gel and in-gel fluorescence were captured by ChemDoc XRS+ (Bio-Rad Laboratories Inc., Hercules, CA, USA), and band intensities were quantified using Image Lab 3.0.1 software (Bio-Rad Laboratories, Inc.).

#### 3.4. Synthesis of a Covalent Aptamer: TBA<sub>3</sub>

TBA<sub>3</sub> with the SO<sub>2</sub>F warhead introduced at the 3rd T residue was synthesized according to the following procedure [16]. Tris(3-hydroxypropyltriazolylmethyl)amine (in water, 0.50  $\mu$ mol, Aldrich, #762342, USA) and copper (II) sulfate (in water, 0.25  $\mu$ mol, Aldrich, #451657, USA) were mixed at a 5  $\mu$ L scale and incubated at room temperature for 5 min. Then, alkyne-containing TBA (T<sub>3</sub>) (in water, 10 nmol), 4-(2-azidoacetyl)-benzene-1-sulfonyl fluoride (in DMSO, 0.50  $\mu$ mol), and ascorbic acid (in water, 0.40  $\mu$ mol, Aldrich, #A92902, USA) were successively added, and the mixture (25  $\mu$ L in total) was reacted for 1 h at 4 °C. The crude reaction product was purified by ethanol precipitation as follows. Sodium acetate (in water, 9  $\mu$ mol) and cold ethanol were added to the crude product and incubated at –20 °C for 1 h. After centrifugation (12,600  $\times$  g, 20 min, 4 °C), the supernatant was removed, and the pellet was washed with 70% ethanol. The residue was dissolved in nuclease-free water.

#### 3.5. Kinetics Evaluation of TBA<sub>3</sub>

Thrombin activity inhibition by TBA<sub>3</sub> was measured using a turbidimetric assay. We mixed various molar concentrations of TBA<sub>3</sub> with a constant molar concentration of thrombin (25  $\mu$ M), with various incubation times in Dulbecco's phosphate-buffered saline (D-PBS) at 37 °C. Then, each reaction mixture was added into fibrinogen solution (in D-PBS) to give a final concentration of 2.5 nM thrombin and 1 mg/mL of fibrinogen, and the maximum absorbance of the polymerized fibrin (288 nm) was measured after three minutes using a nanophotometer (Implen, Munich, Germany) with a 10 mm plastic cell. In each experiment, the maximum absorbance of polymerized fibrin at 0 s was normalized to 0, and the relative absorbance was quantified. The thrombin inhibition denoted as degree of inhibition (DoI), was calculated as the mean  $\pm$  SD (n = 3) from the quantified values and plotted against time. Exponential curve fitting of the plot using GraphPad Prism 6 (GraphPad Software, San Diego, CA, USA) gave us the value of the observed rate constant ( $k_{\text{obs}}$ ) at each TBA<sub>3</sub> concentration via the equation DoI (%) =  $v_i/k_{\text{obs}} \times [1 - \exp(-k_{\text{obs}} \times t)]$ ,

where  $v_i$  = initial velocity (Figure 2B). Finally, the values of  $k_{\text{obs}}$  (i.e., the pseudo-first-order rate constant) were plotted against the TBA<sub>3</sub> concentrations, and the values of  $K_i$  and  $k_{\text{inact}}$  (i.e., the inhibition constant and inactivation rate constant, respectively) were determined by curve fitting of  $k_{\text{obs}} = (k_{\text{inact}} \times [I]) / (K_i + [I])$ ;  $[I]$  = TBA<sub>3</sub> concentration (Figure 2C).

### 3.6. Evaluation of Nuclease Resistance by Liquid Chromatography or Gel Electrophoresis

Unmodified TBA or TBA<sub>3</sub> (0.10 mM) was mixed with thrombin (25  $\mu\text{M}$ ) in D-PBS and incubated for 3 h at 37 °C. Then, human serum was added to 40% ( $v/v$ ) and further incubated for 24 h at 37 °C. The reaction mixture was heated at 95 °C for 10 min and centrifuged at 10,000 $\times g$  for 10 min. The supernatant was analyzed by HPLC (Figure 3A). For the gel electrophoresis analysis, Sample Buffer (Wako, #198-13282, Osaka, Japan) supplemented with 2-mercaptoethanol was added to the reaction mixture, and the mixture was separated by 12% sodium dodecyl sulfate-polyacrylamide gel electrophoresis (SDS-PAGE). Whole proteins were visualized using Coomassie brilliant blue (CBB) staining (Figure 3B). For the assessment of specific nuclease resistance, ten units of specific nuclease (S1 nuclease, Exonuclease VII, or DNase I) were added instead of the serum (Figure 4).

### 3.7. Evaluation of Nuclease Resistance of TBA<sub>3</sub> after the Addition of the Complementary Strand (CS) by Gel Electrophoresis

Thrombin (25  $\mu\text{M}$ ), with or without TBA<sub>3</sub> (0.10 mM) in D-PBS, was incubated for 3 h at 37 °C. The mixture was supplemented with or without CS (400  $\mu\text{M}$ ) for 30 min at 37 °C. Then, it was mixed with ten units of each nuclease (DNase I, S1 nuclease, Exonuclease VII) for 24 h at 37 °C. Then, as described in the previous procedure (Section 3.6), SDS-PAGE was performed, and whole proteins were visualized by CBB staining (Figure 5).

### 3.8. Evaluation of Thrombin Inhibition Activity in the Presence of Human Serum or Nucleases

For the assessment of thrombin inhibition activity, TBA or TBA<sub>3</sub> (0.10 mM) was mixed with thrombin (25  $\mu\text{M}$ ) in D-PBS and incubated for 3 h at 37 °C. Then, ten units of either DNase I or Exonuclease VII, or 40% ( $v/v$ ) human serum was added. The mixture was further incubated for 24 h at 37 °C. The thrombin activity of each reaction mixture was analyzed using a turbidimetric assay. Each reaction mixture was added into the fibrinogen solution (in D-PBS) to give a final concentration of 2.5 nM thrombin and 1 mg/mL of fibrinogen. The maximum absorbance of polymerized fibrin (288 nm) was measured after three minutes using the nanophotometer. In each experiment, the maximum absorbance of polymerized fibrin at 0 s was normalized to 0, and the relative absorbance was quantified (Figure 6).

## 4. Conclusions

In conclusion, we demonstrated a novel method of endowing a DNA aptamer with nuclease resistance. TBA<sub>3</sub> formed a permanent bond to thrombin, resulting in a drug-protein complex that was not affected by the classical equilibrium kinetics of binding (i.e.,  $K_D = 0$ ). As a result, TBA<sub>3</sub> showed a long-term relative resistance against nucleases and maintained the desired thrombin inhibition activity. While we did not examine the *in vivo* pharmacokinetics of TBA<sub>3</sub>, a prolonged inhibition of the target protein is expected from the extension of the pharmacological half-life due to the covalent binding, regardless of the macroscopically observable pharmacokinetic half-life of the free TBA<sub>3</sub>. For *in vivo* applications, the relatively slow covalent bond formation by TBA<sub>3</sub> could be easily overcome by a continuous infusion, to maintain an adequate serum concentration analogous to other short-acting drugs. We believe these advantages provided by the covalently binding aptamer will mitigate the major obstacles to the therapeutic application of aptamers, such as susceptibility to hydrolysis by nucleases and rapid clearance through glomerular filtration, while maintaining the highly desirable property of a reversible covalent drug, and will speed up the translation of aptamer therapeutics to clinical applications.

**Supplementary Materials:** The following supporting information can be downloaded at: <https://www.mdpi.com/article/10.3390/ijms23147778/s1>. References [34,35] are cited in the supplementary materials.

**Author Contributions:** Conceptualization, Y.T., J.Y. and M.T.; methodology, Y.T., J.Y. and M.T.; validation, Y.T.; formal analysis, Y.T.; investigation, Y.T.; resources, Y.T., J.Y. and M.T.; data curation, Y.T.; writing—original draft preparation, Y.T.; writing—review and editing, J.Y. and M.T.; visualization, Y.T.; supervision, Y.T., J.Y. and M.T.; project administration, Y.T., J.Y. and M.T.; funding acquisition, Y.T. and M.T. All authors have read and agreed to the published version of the manuscript.

**Funding:** This research was funded by a JSPS KAKENHI grant (grant numbers #20J22890, #21K05287, #21K12123), and an internal UEC grant for promoting research integration (originating from MEXT, the program for promoting the enhancement of research universities) (grant number not applicable).

**Data Availability Statement:** The data presented in this study are available on request from the corresponding author. The data are not publicly available due to privacy restrictions.

**Acknowledgments:** We thank our colleagues, especially S. Watanabe and N. Miyashita, and the members of the Taki Laboratory for many discussions and suggestions. We thank N. Tomoda (Department GI Surg 2, Hokkaido University Graduate School of Medicine) for assistance with Figure S2.

**Conflicts of Interest:** The authors declare no conflict of interest.

## References

1. Kasahara, Y.; Kuwahara, M. Artificial specific binders directly recovered from chemically modified nucleic acid libraries. *J. Nucleic Acids* **2012**, *2012*, 156482. [[CrossRef](#)] [[PubMed](#)]
2. Rusconi, C.P.; Scardino, E.; Layzer, J.; Pitoc, G.A.; Ortel, T.L.; Monroe, D.; Sullenger, B.A. RNA aptamers as reversible antagonists of coagulation factor IXa. *Nature* **2002**, *419*, 90–94. [[CrossRef](#)] [[PubMed](#)]
3. Odeh, F.; Nsairat, H.; Alshaer, W.; Ismail, M.A.; Esawi, E.; Qaqish, B.; Bawab, A.A.; Ismail, S.I. Aptamers chemistry: Chemical modifications and conjugation strategies. *Molecules* **2019**, *25*, 3. [[CrossRef](#)]
4. Bompiani, K.M.; Woodruff, R.S.; Becker, R.C.; Nimjee, S.M.; Sullenger, B.A. Antidote control of aptamer therapeutics: The road to a safer class of drug agents. *Curr. Pharm. Biotechnol.* **2012**, *13*, 1924–1934. [[CrossRef](#)]
5. Adachi, T.; Nakamura, Y. Aptamers: A review of their chemical properties and modifications for therapeutic application. *Molecules* **2019**, *24*, 4229. [[CrossRef](#)]
6. Chen, X.; Qiu, L.; Cai, R.; Cui, C.; Li, L.; Jiang, J.H.; Tan, W. Aptamer-directed protein-specific multiple modifications of membrane glycoproteins on living cells. *ACS Appl. Mater. Interfaces* **2020**, *12*, 37845–37850. [[CrossRef](#)]
7. Zhang, Y.; Lai, B.S.; Juhas, M. Recent advances in aptamer discovery and applications. *Molecules* **2019**, *24*, 941. [[CrossRef](#)]
8. Byun, J. Recent progress and opportunities for nucleic acid aptamers. *Life* **2021**, *11*, 193. [[CrossRef](#)]
9. Ni, S.; Yao, H.; Wang, L.; Lu, J.; Jiang, F.; Lu, A.; Zhang, G. Chemical modifications of nucleic acid aptamers for therapeutic purposes. *Int. J. Mol. Sci.* **2017**, *18*, 1683. [[CrossRef](#)]
10. Tivon, Y.; Falcone, G.; Deiters, A. Protein labeling and crosslinking by covalent aptamers. *Angew. Chem.* **2021**, *60*, 15899–15904. [[CrossRef](#)]
11. Smith, S.E.; Papavassiliou, A.G. A coupled Southwestern-DNase I footprinting assay. *Nucleic Acids Res.* **1992**, *20*, 5239–5240. [[CrossRef](#)]
12. Galas, D.J.; Schmitz, A. DNase footprinting: A simple method for the detection of protein-DNA binding specificity. *Nucleic Acids Res.* **1978**, *5*, 3157–3170. [[CrossRef](#)] [[PubMed](#)]
13. Wang, X.L.; Li, F.; Su, Y.H.; Sun, X.; Li, X.B.; Schluesener, H.J.; Tang, F.; Xu, S.Q. Ultrasensitive detection of protein using an aptamer-based exonuclease protection assay. *Anal. Chem.* **2004**, *76*, 5605–5610. [[CrossRef](#)] [[PubMed](#)]
14. Liu, Y.; Wang, C.; Li, F.; Shen, S.; Tyrrell, D.L.; Le, X.C.; Li, X.F. DNase-mediated single-cycle selection of aptamers for proteins blotted on a membrane. *Anal. Chem.* **2012**, *84*, 7603–7606. [[CrossRef](#)] [[PubMed](#)]
15. Hu, H.W.; Ding, Y.J.; Gao, Z.H.; Li, H. S1 nuclease digestion-based rational truncation of PD-L1 aptamer and establishment of a signal dual amplification aptasensor. *Sens. Actuators B Chem.* **2021**, *331*, 129442. [[CrossRef](#)]
16. Tabuchi, Y.; Yang, J.; Taki, M. Inhibition of thrombin activity by a covalent-binding aptamer and reversal by the complementary strand antidote. *Chem. Commun.* **2021**, *57*, 2483–2486. [[CrossRef](#)]
17. Zheng, Q.; Woehl, J.L.; Kitamura, S.; Santos-Martins, D.; Smedley, C.J.; Li, G.; Forli, S.; Moses, J.E.; Wolan, D.W.; Sharpless, K.B. SuFEx-enabled, agnostic discovery of covalent inhibitors of human neutrophil elastase. *Proc. Natl. Acad. Sci. USA* **2019**, *116*, 18808–18814. [[CrossRef](#)]
18. Dong, J.; Krasnova, L.; Finn, M.G.; Sharpless, K.B. Sulfur(VI) fluoride exchange (SuFEx): Another good reaction for click chemistry. *Angew. Chem.* **2014**, *53*, 9430–9448. [[CrossRef](#)]
19. Barrow, A.S.; Smedley, C.J.; Zheng, Q.; Li, S.; Dong, J.; Moses, J.E. The growing applications of SuFEx click chemistry. *Chem. Soc. Rev.* **2019**, *48*, 4731–4758. [[CrossRef](#)]

20. Narayanan, A.; Jones, L.H. Sulfonyl fluorides as privileged warheads in chemical biology. *Chem. Sci.* **2015**, *6*, 2650–2659. [[CrossRef](#)]
21. Mukherjee, H.; Debreczeni, J.; Breed, J.; Tentarelli, S.; Aquila, B.; Dowling, J.E.; Whitty, A.; Grimster, N.P. A study of the reactivity of S-(VI)-F containing warheads with nucleophilic amino-acid side chains under physiological conditions. *Org. Biomol. Chem.* **2017**, *15*, 9685–9695. [[CrossRef](#)] [[PubMed](#)]
22. Yang, B.; Wang, N.; Schnier, P.D.; Zheng, F.; Zhu, H.; Polizzi, N.F.; Ittuveetil, A.; Saikam, V.; DeGrado, W.F.; Wang, Q.; et al. Genetically introducing biochemically reactive amino acids dehydroalanine and dehydrobutyrine in proteins. *J. Am. Chem. Soc.* **2019**, *141*, 7698–7703. [[CrossRef](#)] [[PubMed](#)]
23. Xu, R.; Xu, T.; Yang, M.; Cao, T.; Liao, S. A rapid access to aliphatic sulfonyl fluorides. *Nat. Commun.* **2019**, *10*, 3752. [[CrossRef](#)]
24. Shishido, Y.; Tomoike, F.; Kimura, Y.; Kuwata, K.; Yano, T.; Fukui, K.; Fujikawa, H.; Sekido, Y.; Murakami-Tonami, Y.; Kameda, T.; et al. A covalent G-site inhibitor for glutathione S-transferase Pi (GSTP1-1). *Chem. Commun.* **2017**, *53*, 11138–11141. [[CrossRef](#)]
25. Baillie, T.A. Targeted covalent inhibitors for drug design. *Angew. Chem.* **2016**, *55*, 13408–13421. [[CrossRef](#)] [[PubMed](#)]
26. Gan, J.; Zhang, H.; Humphreys, W.G. Drug-protein adducts: Chemistry, mechanisms of toxicity, and methods of characterization. *Chem. Res. Toxicol.* **2016**, *29*, 2040–2057. [[CrossRef](#)]
27. Smith, A.J.; Zhang, X.; Leach, A.G.; Houk, K.N. Beyond picomolar affinities: Quantitative aspects of non-covalent and covalent binding of drugs to proteins. *J. Med. Chem.* **2009**, *52*, 225–233. [[CrossRef](#)]
28. Johnson, D.S.; Weerapana, E.; Cravatt, B.F. Strategies for discovering and derisking covalent, irreversible enzyme inhibitors. *Future Med. Chem.* **2010**, *2*, 949–964. [[CrossRef](#)]
29. Lagoutte, R.; Patouret, R.; Winssinger, N. Covalent inhibitors: An opportunity for rational target selectivity. *Curr. Opin. Chem. Biol.* **2017**, *39*, 54–63. [[CrossRef](#)]
30. Singh, J.; Petter, R.C.; Baillie, T.A.; Whitty, A. The resurgence of covalent drugs. *Nat. Rev. Drug Discov.* **2011**, *10*, 307–317. [[CrossRef](#)]
31. Bauer, R.A. Covalent inhibitors in drug discovery: From accidental discoveries to avoided liabilities and designed therapies. *Drug Discov. Today* **2015**, *20*, 1061–1073. [[CrossRef](#)] [[PubMed](#)]
32. Copeland, R.E. *Evaluation of Enzyme Inhibitors in Drug Discovery: A Guide for Medicinal Chemists and Pharmacologists*, 2nd ed.; John Wiley & Sons, Inc.: Hoboken, NJ, USA, 2013.
33. Schwartz, P.A.; Kuzmic, P.; Solowiej, J.; Bergqvist, S.; Bolanos, B.; Almaden, C.; Nagata, A.; Ryan, K.; Feng, J.; Dalvie, D.; et al. Covalent EGFR inhibitor analysis reveals the importance of reversible interactions to potency and mechanisms of drug resistance. *Proc. Natl. Acad. Sci. USA* **2014**, *111*, 173–178. [[CrossRef](#)] [[PubMed](#)]
34. Crisafuli, F.A.P.; Ramos, E.B.; Rocha, M.S. Characterizing the interaction between DNA and GelRed fluorescent stain. *Eur. Biophys. J. Biophys. Lett.* **2015**, *44*, 1–7. [[CrossRef](#)] [[PubMed](#)]
35. Hirasawa, S.; Kitahara, Y.; Okamatsu, Y.; Fujii, T.; Nakayama, A.; Ueno, S.; Ijichi, C.; Futaki, F.; Nakata, K.; Taki, M. Facile and Efficient Chemoenzymatic Semisynthesis of Fc-Fusion Compounds for Half-Life Extension of Pharmaceutical Components. *Bioconjug. Chem.* **2019**, *30*, 2323–2331. [[CrossRef](#)] [[PubMed](#)]